

Measurements of Seismometer Orientation at USArray Transportable Array and Backbone Stations

Göran Ekström

Lamont-Doherty Earth Observatory of Columbia University, Palisades, NY

Robert W. Busby

Incorporated Research Institutions for Seismology, Washington, DC

INTRODUCTION

Modern broadband seismometers generally have well-known and stable instrument parameters. Typically, the manufacturer's specifications indicate that the gain of each component of a three-component seismometer is known to within 1% and that the orthogonality of the components is true to within a fraction of a degree. Such precision makes possible many types of quantitative seismological analyses that were difficult with earlier instruments. In particular, different components of earlier three-component seismometers did not necessarily have the same response functions (*e.g.*, free period of the seismometer), making any analysis based on the rotation of ground motion into the transverse and longitudinal directions difficult. Such technical problems have now largely been overcome in the most common broadband instrumentation, and it is routine to perform rotational transformations of the horizontal components of motion in modern seismological analyses, such as earthquake source investigations, *S* and *SKS* splitting studies, receiver-function determinations, and body- and surface-wave-polarization studies.

An essential station variable for the rotational transformation of horizontal components of motion is the geographical orientation of the original components in the horizontal plane. Horizontal seismometers are typically installed with output sensitivity aligned to the north-south and east-west directions, and the standard names of seismometer channels (*e.g.*, BHN, BHE) reflect this convention. Nontraditional orientations are common for borehole and ocean-bottom seismometers, for which it is cumbersome or impossible to install the seismometer with a specified orientation, and the orientation is instead determined after deployment. In general, instruments with nontraditional orientations have channel names that reflect this (*e.g.*, BH1, BH2). Regardless of how the seismometer is oriented at installation, the azimuths of sensitivity of the horizontal components

are subsequently distributed as auxiliary data. In the SEED convention, as well as in other data distribution formats, the precision of this parameter is given to at least 0.1°.

Despite the precision with which seismometer orientations are given, the accuracy of the reported azimuths is neither well-known nor easily verified. The uncertainty derives from several factors. It is not easy to orient seismometers in the field. Typically, seismometers are deployed in remote areas and often underground. Obtaining a high-fidelity bearing at the site of installation can be difficult and, even when one is available, ensuring that the seismometer is properly aligned remains a challenge. In addition, many opportunities exist to make mistakes. In particular, when a magnetic compass is used for the alignment, there is frequently a significant site-specific declination correction to be made. Errors are introduced when this correction is not made, when a correction is made in the opposite sense to that required, or when the wrong correction for the location is applied. Obtaining direct measurements of the orientation of the seismometer after installation is associated with the same difficulties and compounded by the presence of strong magnets within the sensor itself. USArray has recently used an IXSEA Octans IV interferometric fiber-optic gyroscope to determine bearings in the field (<http://www.ixsea.com/en/products/002.001.002.001/octans.html>). Measurements of alignment references and actual sensors indicate that determination of the desired orientation is the step most likely to result in errors. Repeated experiments show that alignment of sensors to a chosen reference is a smaller source of error, with repeat alignments deviating from each other by only a few degrees.

Probable errors in the reported orientation of horizontal components have been discussed in several studies of body- and surface-wave polarization. The polarization of the wavefield (*e.g.*, arrival-angle azimuth) provides valuable constraints on isotropic and anisotropic structure along the ray path from an earthquake to a receiver, as well as beneath the receiver, and a

lack of knowledge of the true orientation of the horizontal components complicates the interpretation of polarization observations. Laske (1995) and Laske and Masters (1996) used long-period surface-wave polarization measurements to constrain global phase-velocity variations and found that the instrument orientations at several globally distributed stations were incorrect by more than 5°. Larson (2000) and Larson and Ekström (2002) reached a similar conclusion in a study of polarization of intermediate-period surface waves and reported misorientations of more than 10° for 10 stations of the Global Seismographic Network (GSN). For stations in common with those reported by Laske and Masters (1996), estimated misorientations were found to be very similar. Yoshizawa *et al.* (1999) and Schulte-Pelkum *et al.* (2001) investigated *P*-wave polarizations at GSN stations, and found similar misorientations to those reported in the surface-wave studies.

The results of these studies suggest that robust estimates of sensor orientation can be obtained directly from the recorded waveforms by appropriate averaging or fitting of many polarization measurements. In the current study, we present a simple, automated algorithm for making many long-period polarization measurements and for deriving estimates of sensor orientation from these measurements. We apply the algorithm in a systematic fashion to two years of data from the USArray Transportable Array (TA) and Backbone (BB) stations. An important result from our analysis is that the majority of the stations appear to have true orientations within 0–3° of the reported orientation. For a few stations, however, we find deviations larger than 10°. Errors of this magnitude can confound the geophysical interpretation of polarization measurements and complicate the quantitative analysis of the unique data collected by USArray. Our hope is that this study will motivate efforts to develop and implement methods of documenting the true sensor orientation of USArray and other stations as well as provide a means to estimate orientations of stations no longer deployed.

METHOD

Our analysis is based on measurements of wavefield polarization, in particular the polarization of intermediate- and long-period Love and Rayleigh waves. We selected all earthquakes of $M_w \geq 5.5$ occurring between January 2006 and December 2007 for the analysis. Events of this size are typically well recorded by permanent and temporarily deployed broadband stations in the period range used in the Global CMT analysis (40–250 s). Approximately 400 earthquakes of this size occur each year. The data were collected from networks and stations that are part of the Transportable Array and Backbone components of USArray. Specifically, data from the virtual networks US-TA and US-BB were requested and retrieved from the Incorporated Research Institutions for Seismology (IRIS) Data Management Center in Seattle, Washington. Most of the stations belong to the pool of instruments that are deployed in temporary vaults for a duration of approximately 24 months (network code TA) and are then moved to a new location. Several of the stations are permanent, most belonging to the US National Seismic

Network (US), the Caltech Regional Seismic Network (CI), or the Berkeley Digital Seismic Network (BK). Seismograms from the long-period (LH) channels were used in the analysis and, for stations with more than one sensor, data from all sensors were included. Most of the transportable stations are equipped with a Streckeisen STS-2, Güralp CMG-3T, or Nanometrics Trillium 240 seismometer, while the instrumentation at the permanent stations is more varied, including several sets of vertical and horizontal Streckeisen STS-1 seismometers.

The data were assembled and filtered as for standard CMT analysis (Ekström *et al.* 2005; Ekström, Dalton, and Nettles 2006). An essential step of the processing is the incorporation of auxiliary information associated with the instruments used in the analysis. This includes the instrument response functions and the orientations of the sensors. For all of the data, we used the best information currently available, obtained in the form of “dataless SEED” volumes from the IRIS Data Management Center on 2 January 2008.

The CMT analysis (Dziewonski *et al.* 1981; Dziewonski and Woodhouse 1983) involves matching long-period three-component seismograms in an inversion that results in an estimate of the earthquake moment tensor and its centroid in space and time. Currently, three types of waveforms are used in the CMT analysis: 1) body waves (B), which are the intermediate-period (40–150 s) waveforms that arrive before the fundamental-mode surface waves; 2) mantle waves (M), which are the long-period (125–300 s) waveforms recorded during the first few hours after the earthquake and dominated by long-period, multiple-orbit Love and Rayleigh waves; and 3) surface waves (S), which are the intermediate-period (50–150 s) minor-arc surface-wave arrivals. In the polarization analysis described here, we use measurements derived from the intermediate-period surface-wave waveforms (S) but also make a comparison with measurements obtained from the long-period mantle-wave waveforms (M).

Rather than utilizing the extensive USArray dataset in a separate CMT inversion for the earthquake source, we simply calculate synthetic waveforms corresponding to the published CMT focal mechanism derived from the GSN dataset. The synthetic waveforms are calculated in the same manner as in the standard Global CMT earthquake analysis, using normal-mode summation and surface-wave ray theory, including approximate corrections for Earth’s laterally heterogeneous structure (Dziewonski *et al.* 1984; Arvidsson and Ekström 1998). None of these corrections include effects related to wave refraction away from the great-circle path, and the synthetic seismograms thus have the same polarization characteristics as on a spherically symmetric Earth. The horizontal components of both observed and synthetic waveforms are rotated into the transverse and longitudinal directions, initially using the reported azimuths of the first and second (usually north and east) horizontal components, α_1 and α_2 . Time windows containing the main surface-wave arrivals are automatically selected for analysis based on epicentral distance and noise levels. Correlations C between observed and synthetic transverse and longitudinal components are then calculated,

$$C = \frac{\sum_{i=1}^N o_i s_i}{\sqrt{\sum_{i=1}^N o_i^2 \sum_{i=1}^N s_i^2}},$$

where o_i is the observed time series, N is the number of selected time points, and s_i is the synthetic time series. We then explore the effect on C of varying the orientations of the horizontal components. While, in general, it is possible for these components not to be orthogonal, especially for systems with a separate seismometer for each component (such as the STS-1) we assume here that the relative orientation ($\alpha_2 - \alpha_1$) is constant (90° or -90°), and only investigate the effect of adding the same rotation angle $\delta\alpha$ to both azimuths. This corresponds to a horizontal rotation of the three-component seismometer.

The observed transverse and longitudinal seismograms o_i are recalculated for the new assumed orientations of the horizontal components, $\alpha_1 - \delta\alpha$ and $\alpha_2 - \delta\alpha$, where a positive $\delta\alpha$ corresponds to a counter-clockwise rotation of the seismometer. The correlation values are recalculated as $C_L(\delta\alpha)$ and $C_T(\delta\alpha)$, where the subscripts refer to the longitudinal and transverse directions. We calculate the correlations for a range of orientations $-89^\circ \leq \delta\alpha \leq 90^\circ$ at 1° increments. We define the total correlation C_{tot} for a pair of longitudinal and transverse seismograms as

$$C_{\text{tot}}(\delta\alpha) = \min(|C_L(\delta\alpha)|, |C_T(\delta\alpha)|),$$

and the optimal rotation $\delta\alpha^*$ is the one that produces the largest C_{tot} . C_L^* and C_T^* are then the corresponding correlations for the two seismogram components. An additional parameter related to the correlation is the scaling factor S , which is the factor by which the synthetic seismogram should be multiplied in order to achieve the smallest residual variance between the observed and synthetic waveforms,

$$S = \frac{\sum_{i=1}^N o_i s_i}{\sum_{i=1}^N s_i^2}.$$

S_L^* and S_T^* are the scaling factors that correspond to the optimal rotation $\delta\alpha^*$.

The algorithm described above was chosen to generate robust average polarization angles and is not optimal for measuring the polarization of an individual Rayleigh or Love wave. In particular, the total correlation depends on the correlations of both wave types, and the derived polarization angle may not be representative of either wave when, for example, their ray paths deviate in different ways from the great-circle path. In addition, the total correlation will not be very large if either the Love or Rayleigh wave is nodal, since the correlation of the nodal component will be more strongly influenced by noise.

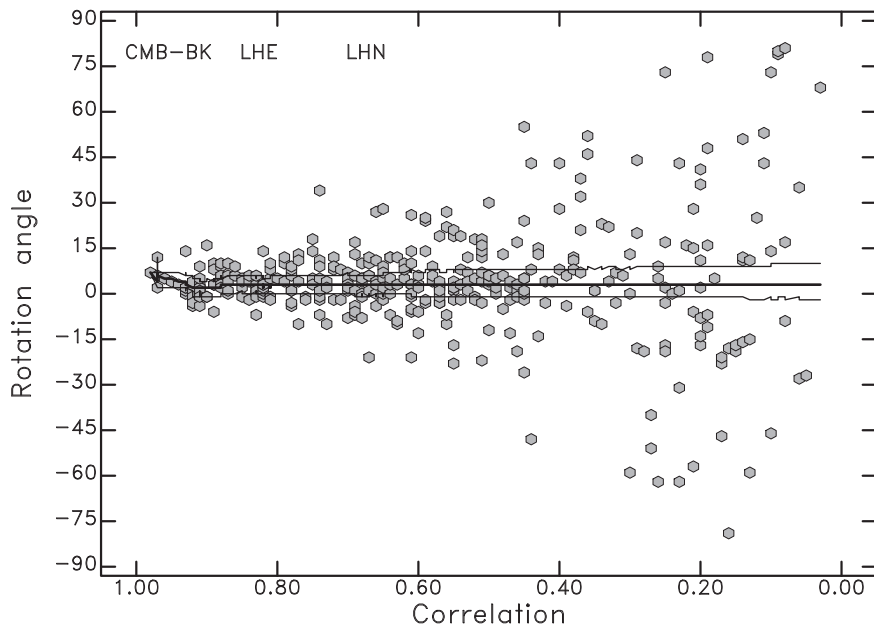
The polarization measurements are affected by several factors, including geophysically interesting ones, such as refraction of the wave during propagation and anisotropy in the receiver region, and less interesting ones, such as station misorientation, different gain errors on horizontal components, and noise. Of these sources, only the station misorientation will make a constant contribution to the polarization angle for all arrivals, regardless of azimuth. In the second part of the analysis, for each station, the optimal rotation angles $\delta\alpha^*$ obtained from many earthquakes are used to calculate a median rotation angle, which we take to represent the station orientation. The range of the second and third quartiles of the distribution of measurements of $\delta\alpha^*$ is calculated to provide an uncertainty estimate for the estimated orientation.

RESULTS

A total of 973 earthquakes were processed, and 518 USArray stations were included in the analysis. At a small number of the permanent stations, more than one seismometer is operating, identified by a distinct location code or distinct channel names. In these cases, data from all sensors were included, for a total number of distinct seismometers of 530. In addition, seismometers at some stations have been replaced or reinstalled. In what follows, the distinction between a station, a seismometer, and a seismometer epoch will be made only when necessary; in general we will refer to "a station."

Synthetic seismograms were calculated for all stations for which a real seismogram was recorded, but for many of the smaller earthquakes the signal level was too small to obtain a significant correlation with the synthetic waveforms, especially at some of the noisier stations. Only measurements corresponding to highly correlated traces are useful for the polarization analysis. We therefore make a quality selection of the available measurements based on the correlation coefficients C_L and C_T , and also make a selection based on epicentral distance and earthquake focal depth. For the intermediate-period surface waves (S data), we discard all measurements corresponding to paths shorter than 15° and all measurements corresponding to earthquakes deeper than 100 km. For the long-period surface waves (M data), we discard measurements corresponding to paths shorter than 45° but make no selection based on earthquake depth. In addition, we discard all measurements associated with scaling factors S_L^* or S_T^* greater than 2.0 or smaller than 0.5.

The choice of a selection criterion based on the value of the correlation C_{tot} is guided by several considerations. A higher correlation is presumably indicative of a better polarization measurement, but it is important to include several measurements in order to average out observational errors and potentially anomalous azimuths or paths. Figure 1 shows an example of the distribution of measured angles $\delta\alpha^*$ as a function of correlation C_{tot} for a low-noise station. Measurements corresponding to higher correlation values are in general consistent, with a greater scatter for smaller correlation values. We calculate the median of the observations using different minimum cut-off



▲ **Figure 1.** Individual measurements of polarization angle $\delta\alpha^*$ as a function of the corresponding optimal combined correlation coefficient C_{tot} for the station CMB-BK. The thick line shows the median of the individual measurements above a given correlation coefficient, and the thin lines show the range of the second and third quartiles of this distribution of measurements.

values for the correlation and show the median as a function of this value in figure 1. The median does not vary much after ~ 10 measurements have been included in the calculation, and is thus quite robust. The effect of using a lower cutoff value is therefore not large for stations with low noise levels and many available high-correlation measurements. For noisy stations, where high-correlation measurements seldom are obtained, a high cut-off value would, however, lead to very few accepted measurements. Based on results from extensive experimentation, we chose a cut-off value for C_{tot} of 0.60. This choice leads to 89% of the stations in our dataset generating at least 10 acceptable measurements.

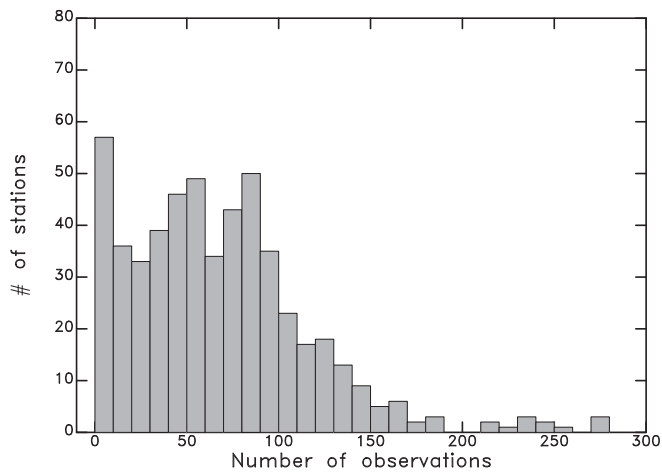
Since global seismicity levels are relatively stable, the number of acceptable measurements will mostly be determined by the duration of operation of the station and the level of the background horizontal noise. Since many of the TA stations were installed during the second half of 2007, there are several stations for which only a limited number of measurements are available. Figure 2 shows the distribution of the number of measurements that result when we apply the selection criteria described above. For some of the quietest stations, we have more than 200 measurements for the two-year period. The largest number of measurements, 277, was obtained from the JCC-BK and DUG-US stations. For 57 stations we obtained fewer than 10 measurements. For most of these (52), the period of available data was less than four months. For the remaining five stations (CNNC-US, GOGA-US, EGMT-US, P19A-TA, SDP-CI), the lack of success of our method is not clear. In the following analysis, we include only those stations for which 10 or more acceptable measurements were obtained.

Our estimate of the orientation of the horizontal components is calculated as the median of all acceptable polarization

measurements for a station. The orientation is presented as a correction angle that should be subtracted from the reported angle to obtain the azimuth of sensitivity of the sensor. Figure 3 shows the distribution of correction angles for the 473 stations. The distribution is closely centered around 0° and 75.9% of the correction angles lie in the range -3° to $+3^\circ$. It should be stressed that there is nothing in the measurement technique that favors angles close to the reported orientation. The tails of the distribution are more prominent than for a normal distribution, with 13.7% of the correction angles falling between 4° and 6° and 10.3% of the angles deviating by 7° or more from the reported orientation.

Table 1 shows the statistics of the distribution for all the stations as well as for the four individual networks (TA, US, CI, BK). Our analysis indicates that the stations of the Berkeley network are unusually well oriented; for only two of the 20 stations do we obtain correction angles larger than 3° . The TA stations have estimated orientations that are more consistent with the reported orientations than the stations of the permanent networks (US, CI, BK), taken as a group. All networks, except for the BK network, have several stations with measured orientations that deviate by more than 10° from the reported values.

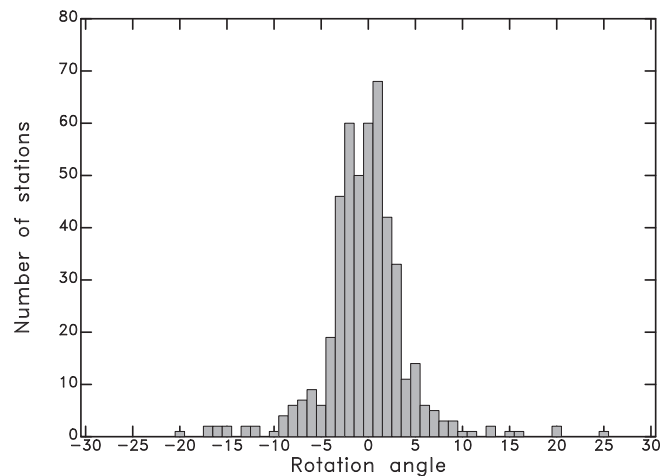
It is difficult to calculate a useful uncertainty for our orientation estimates, since we expect most of the factors that influence the polarization measurement to be systematic, rather than random. For example, if refraction across the western margin of North America causes a significant deviation of ray paths from the western Pacific, the influence of this signal on the distribution of measurements will depend on the distribution of earthquakes at different azimuths from the station. Similarly, if there is a gain error on one of the horizontal components, the influence on the median deviation will depend on the azimuthal



▲ **Figure 2.** Histogram showing the distribution of the number of polarization measurements that satisfy the selection criteria. The ranges are 0–9, 10–19, 20–29, etc., and the maximum number of polarization measurements obtained for a single station is 277.

distribution of earthquakes. Rather than devising an algorithm to attempt to account for these factors, we present the range of observations defined by the second and third quartiles of the measurements for each station. The median range for the 473 stations is approximately 10°. Figure 4 shows the estimated correction angle and the associated uncertainty range for those stations that have correction angles that are greater than 6°. Only for three of these stations do the uncertainty ranges span 0°.

In addition to the rotation angles determined from the intermediate-period surface waves (S), we determined a second set of angles using the longer-period mantle waves (M). Because these longer-period waves are excited well only by large earthquakes, we obtain a smaller number of measurements from these data. Figure 5 shows a comparison between the two data-sets for the 430 stations for which we obtained rotation-angle estimates using both types of data. The consistency of the two measurements is good, with few observations differing by more than 4°. The uncertainty in the M measurements is greater, and we do not at this time have an explanation for the apparent 1° offset between the two sets of observations. For these reasons, we chose not to combine the data sets, and base our preferred results only on the intermediate-period measurements.



▲ **Figure 3.** Histogram showing the distribution of rotation angles for 473 USArray stations.

The results for all of the stations analyzed in this study are available in tabular format at <http://www.ldeo.columbia.edu/~ekstrom/Research/SRL2008>.

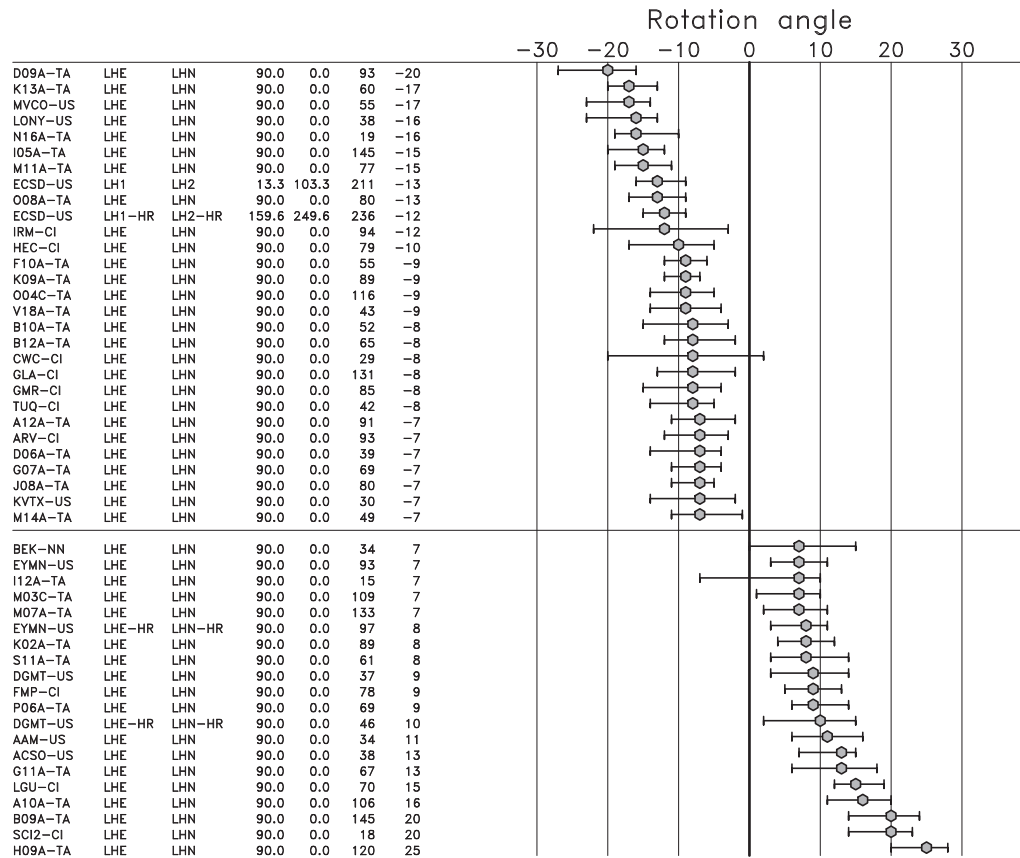
DISCUSSION

Some preliminary results from this study were available in mid-2007. In particular, it became clear that some of the Transportable Array stations appeared to be misoriented, based on our surface-wave-polarization analysis, by more than 10° with respect to the reported orientation. This observation caused concern, especially since the stations were scheduled to be dismantled and removed within 12 months. Without further effort, the potential misorientation of the instrument would not be verifiable, and the true orientation of the instrument would not be known. IRIS obtained a new gyroscope tool, the IXSEA Octans IV interferometric fiber-optic gyroscope (see figure 6), for obtaining precise and accurate measurements of azimuths in the field, and this tool is now used to determine the seismometer orientations at TA stations at the time of deployment and removal. Figure 7 shows a comparison between the polarization- and gyroscope-based estimates of the seismometer orientation at the first 49 stations for which field measurements have been made. The agreement between the two measurements is

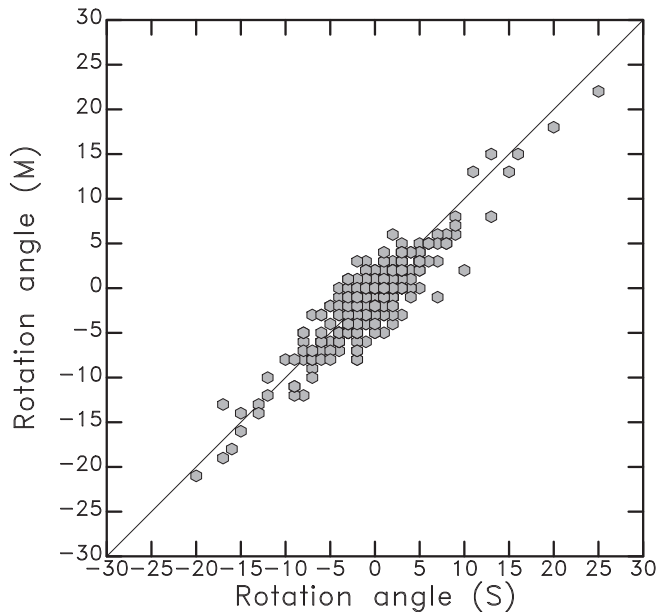
TABLE 1
Statistics of sensor-rotation angles estimated in this study.

Network	# Obs.	0°–3°	4°–6°	7°–9°	10°–90°
All	473	75.9% (359)	13.7% (65)	5.9% (28)	4.4% (21)
TA	364	79.9% (291)	12.6% (46)	4.7% (17)	2.7% (10)
US	43	55.8% (24)	18.6% (8)	9.3% (4)	16.3% (7)
CI	41	56.1% (23)	19.5% (8)	14.6% (6)	9.8% (4)
BK	20	90.0% (18)	10.0% (2)	0.0% (0)	0.0% (0)
Other ^a	5	60.0% (3)	20.0% (1)	20.0% (1)	0.0% (0)

a. These five stations are from the AZ and NN networks.



▲ **Figure 4.** Figure showing the rotation angle and corresponding estimated uncertainty for the 49 stations with rotation angles deviating by 7° or more from the reported orientations. The columns on the left give the station code, the channel names of the two horizontal components, the reported azimuths of these two components, the number of acceptable polarization measurements used in the analysis, and the rotation angle.



▲ **Figure 5.** Comparison of rotation angles obtained from the intermediate-period surface waves (S) and those obtained from long-period mantle waves (M). Four hundred and thirty stations are shown.

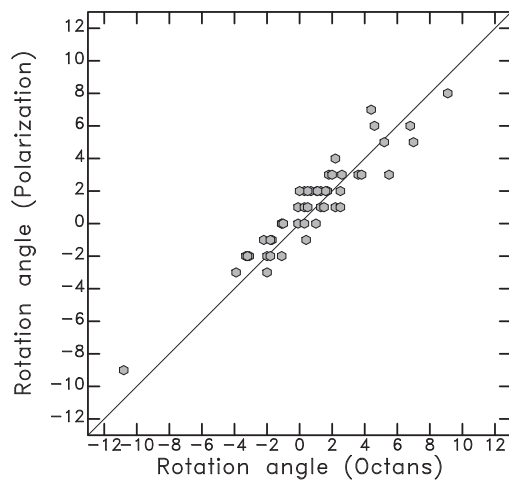
surprisingly good. The root mean square (rms) deviation of the polarization measurement from the gyroscope measurement is 1.2°, which compares favorably with an rms deviation of 3.3° between the reported and gyroscope-based orientations. For no station is the deviation between the polarization- and gyroscope-based orientations greater than 3°. It should be noted that those stations for which the gyroscopic measurements were made had been installed the longest and therefore had the largest number of polarization measurements available.

The good agreement between the field-based and seismogram-based estimates suggests that the true errors in our estimated rotation angles are small. If the errors followed a normal distribution, we would infer that we could estimate the orientation with an error of less than 4° for 99% of the stations, or that only four or five of our 473 estimates would be wrong by more than 4°. While we doubt the accuracy is this high, owing to a host of nonrandom error sources, the evidence suggests that for most of the stations (with the exception of the BK network), the orientation estimate obtained directly from the data is more accurate than the reported orientation.

Current practice in the operation of the USArray Transportable Array is to make a high-precision gyroscope measurement of the seismometer orientation at both installation and removal. This will, presumably, eliminate the future



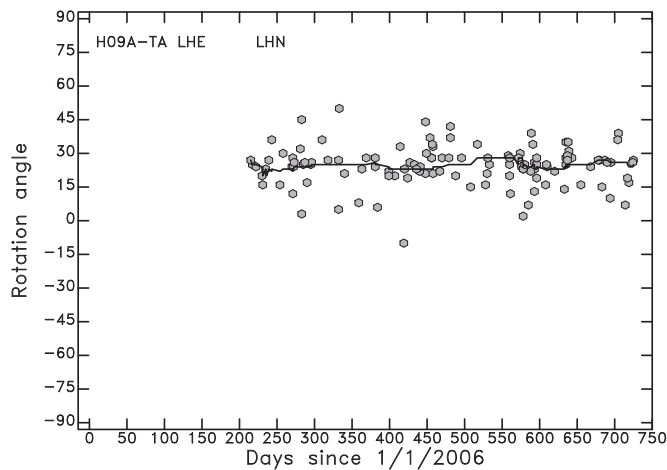
▲ **Figure 6.** Octans device aligned with an STS-2 within a TA station vault. The small size and insensitivity to magnetic influences of this device are key advantages for performing in-situ measurements of sensors. The device determines orientation with respect to the rotation axis of the Earth within 10 minutes. (Photo: R. W. Busby.)



▲ **Figure 7.** Comparison between two types of measurements of rotation angle. The horizontal axis corresponds to high-precision field measurements of seismometer orientation obtained at 49 TA sites at the time of station removal. The measurements were obtained using an IXSEA Octans IV interferometric fiber-optic gyroscope. The vertical axis corresponds to the rotation angle obtained from the surface-wave-polarization measurements. The thin line indicates equal values of the two measurements. The difference between the two measurements is less than 3° for all stations.

need to estimate the orientation from the seismic data. The polarization-angle method will, however, continue to be useful for verifying the orientations of stations belonging to other broadband seismographic networks for which high-precision field measurements are not available. This could include permanent networks as well as temporary PASSCAL-type deployments.

A surprising result from the current study is that a robust estimate of sensor orientation can be obtained relatively quickly. We chose 10 acceptable measurements as our threshold for defining a median orientation. Figure 8 shows the distribution of polarization measurements since installation for the TA station H09A, a station that we find to be misoriented by more than 20° . Also shown in figure 8 is the estimate of the misorientation based on the preceding 20 polarization measurements. That is, the figure shows how the polarization measurement would have changed as a function of time if it were based on only the most recent 20 measurements. While the median value calculated in this manner varies by a few degrees over time, it is clear that 20 measurements is a sufficient number to provide a relatively robust estimate of the true sensor orientation. At stations with noise levels similar to those observed at Transportable Array sites, this number of measurements would typically be obtained in less than four months of recording.



▲ **Figure 8.** Rotation-angle measurements as a function of time for the TA station H09A. The thick line shows the median of the preceding 20 measurements (or fewer, immediately following deployment). The misorientation of the station is evident after only a few measurements are available.

CONCLUSIONS

A number of previous studies (Laske 1995; Laske and Masters 1996; Yoshizawa *et al.* 1999; Larson 2000; Schulte-Pelkum *et al.* 2001; Larson and Ekström 2002) have derived estimates of sensor orientation from data analyses otherwise focused on geophysically interesting signals. This paper describes a simple method for routinely forming such estimates from archived data, with a stable estimate obtained from an observational period as short as four months. As an important validation of our seismogram-derived estimates, we measured the actual sensor orientations with a precision interferometric fiber-optic gyrocompass at 49 Transportable Array stations. The seismogram-derived estimates agree with the gyroscope-measured orientations to within a root mean square (rms) deviation of 1.2° . This deviation is significantly smaller than the 3.3° rms deviation obtained between the reported and gyroscope-derived orientations at these stations. While the use of high-precision orientation devices in the routine installation and decommissioning of TA stations, adopted in 2007, is likely to have resulted in much smaller orientation errors in recent deployments, the seismogram-based methodology described here provides an alternative means of deriving true sensor orientations for stations and networks where direct high-precision sensor-orientation measurements are not available. ☒

ACKNOWLEDGMENTS

We thank Joseph Steim, Frank Vernon, Erhard Wielandt, and Meredith Nettles for helpful discussions. This work was funded by the National Science Foundation, Award EAR-0710842, and an IRIS subaward supporting the Waveform Quality Center at Lamont.

REFERENCES

- Arvidsson, R., and G. Ekström (1998). Global CMT analysis of moderate earthquakes, $MW \geq 4.5$, using intermediate-period surface waves. *Bulletin of the Seismological Society of America* **88**, 1,003–1,013.
- Dziewonski, A. M., and J. H. Woodhouse (1983). An experiment in the systematic study of global seismicity: Centroid-moment tensor solutions for 201 moderate and large earthquakes of 1981. *Journal of Geophysical Research* **88**, 3,247–3,271.
- Dziewonski, A. M., T.-A. Chou, and J. H. Woodhouse (1981). Determination of earthquake source parameters from waveform data for studies of global and regional seismicity. *Journal of Geophysical Research* **86**, 2,825–2,853.
- Dziewonski, A. M., J. E. Franzen, and J. H. Woodhouse (1984). Centroid-moment tensor solutions for January–March 1984. *Physics of the Earth and Planetary Interiors* **34**, 209–219.
- Ekström, G., C. A. Dalton, and M. Nettles (2006). Observations of time-dependent errors in long-period instrument gain at global seismic stations. *Seismological Research Letters* **77**, 12–22.
- Ekström, G., A. M. Dziewonski, N. N. Maternovskaya, and M. Nettles (2005). Global seismicity of 2003: Centroid-moment tensor solutions for 1,087 earthquakes. *Physics of the Earth and Planetary Interiors* **148**, 327–351.
- Larson, E. W. F. (2000). Measuring refraction and modeling velocities of surface waves. PhD dissertation, Harvard University, Cambridge, Massachusetts.
- Larson, E. W. F., and G. Ekström (2002). Determining surface wave arrival angle anomalies. *Journal of Geophysical Research* **107**, doi:10.1029/2000JB000048.
- Laske, G. (1995). Global observation of off-great-circle propagation of long-period surface waves. *Geophysical Journal International* **123**, 245–259.
- Laske, G., and G. Masters (1996). Constraints on global phase velocity maps from long-period polarization data. *Journal of Geophysical Research* **101**, 16,059–16,075.
- Schulte-Pelkum, V., G. Masters, and P. M. Shearer (2001). Upper mantle anisotropy from long-period *P* polarization. *Journal of Geophysical Research* **106**, 21,917–21,934.
- Yoshizawa, K., K. Yomogida, and S. Tsuboi (1999). Resolving power of surface wave polarization data for higher-order heterogeneities. *Geophysical Journal International* **138**, 205–220.

Lamont-Doherty Earth Observatory of Columbia University
 61 Route 9W
 Palisades, New York 10964, U.S.A.
 ekstrom@ldeo.columbia.edu
 (G.E.)